Original Research

Apparent Wall Thickening of Cystic Renal Lesions on MRI

Vikas Gulani, MD, PhD,[1]* Saroja Adusumilli, MD,[2] Hero K. Hussain, MD,[2] Alberto L. Vazquez, PhD,[3] Isaac R. Francis, MD,[2] and Douglas C. Noll, PhD[2,4]

Purpose: To show that cystic renal lesions that would otherwise meet criteria for simple cysts can demonstrate perceptible walls or increased wall thickness on MRI, sometimes causing these lesions to be "upgraded." It was hypothesized that thickening of cyst walls on MRI can be artifactual, due to data truncation, applied filtering, and low signal-to-noise ratio (SNR).

Materials and Methods: k-Space data for a 4-cm cyst were created in a 40-cm field of view (FOV) (512 × 512 matrix). Additional data sets were created using the central 512 × 256 and 512 × 128 points. Noise was simulated so that the cyst SNR was approximately 7, 14, and 20, respectively. Actual wall thickness was set at 0.25 mm, and cyst:wall signal at 1:4. An inverse two-dimensional (2D) fast Fourier transform (FFT) yielded simulated images. A Fermi filter was applied to reduce ringing. Images/projections were examined for wall thickening. Seven patients with initially thick-walled cysts on fat-saturated spoiled gradient-echo (FS-SPGR) images were scanned with increasing resolution (256 × 128 and 256 × 256; four patients were also scanned with 512 × 512). Average wall thickness at each resolution was compared using a two-tailed paired Student's *t-test.*

Results: Simulations showed apparent wall thickening at low resolution, improving with higher resolutions. Low SNR and application of the Fermi filter made it difficult to identify ringing as the cause of this thickening. The simulation results were confirmed on seven patients, whose cyst walls proved to be artifactually thickened ($P < 0.01$).

Conclusion: Thickening of cyst walls on MRI can be artifactual. Upon encountering thick-walled cystic renal lesions, high-resolution images can be acquired to exclude apparent thickening.

Key Words: renal cysts; renal cell carcinoma; Bosniak classification; body MRI; renal MRI; wall thickening
J. Magn. Reson. Imaging 2008;28:103–110.

APPROXIMATELY 5% TO 15% OF RENAL CELL CARCINOMA (RCC) cases present as a predominantly cystic mass (1–3). Presently, it is not possible to definitively diagnose some cystic renal masses as malignant or nonmalignant by imaging criteria; the gold standard remains pathology. However, medical imaging plays a key role in the workup of cystic renal masses and categorization into surgical and nonsurgical lesions. The Bosniak classification system has been employed since 1986 for the computed tomography (CT) classification of cystic renal masses (4). With widespread use of body MRI, there has been interest in the application of the criteria in the Bosniak system or something similar for MRI classification of these cystic masses as well (5–9).

One of the criteria for a simple renal cyst in the Bosniak system is the presence of a thin, imperceptible wall (10–12). Cysts that have one or two thin, fine calcifications in their walls or septa, wall thickening >1 mm and hyperdense cysts that are <3 cm in diameter, one-fourth of their walls extending outside the kidney, and do not show enhancement are placed in Category II and are felt to be benign, requiring no further surgical or radiological workup. Cysts that show wall thickening, nodularity, enhancing walls, multiple internal septations, thick or irregular calcifications, and hyperdense lesions that do not fulfill the criteria for Category II lesions, are placed in Category III, and are indeterminate lesions. An addition to the original Bosniak system is Category IIF (F for "follow-up") (13). These lesions do not fit well into either Category II or III and may contain multiple thin septations, or exhibit mild smooth wall thickening. Classification into Category IIF merits further imaging follow-up to ensure that the lesion in question is indeed benign (14). Wall thickness of as little as 2 to 3 mm has been reported as important for the evaluation of these masses (15).

[1]Department of Radiology, Case Western Reserve University, Cleveland, Ohio, USA.
[2]Department of Radiology, University of Michigan, Ann Arbor, Michigan, USA.
[3]University of Pittsburgh, Department of Radiology, Pittsburgh, Pennsylvania, USA.
[4]Department of Biomedical Engineering, University of Michigan, Ann Arbor, Michigan, USA.
Contract grant sponsor: NIH Clinical and Translational Science Award (CTSA); Contract grant number: 1KL2RR024990.
*Address reprint requests to: V.G., MD, PhD, Department of Radiology, University Hospitals of Cleveland, Case Western Reserve University, 11100 Euclid Ave., Cleveland, OH 44106. E-mail: vikas@case.edu
Received July 25, 2007; Accepted February 12, 2008.
DOI 10.1002/jmri.21376
Published online in Wiley InterScience (www.interscience.wiley.com).

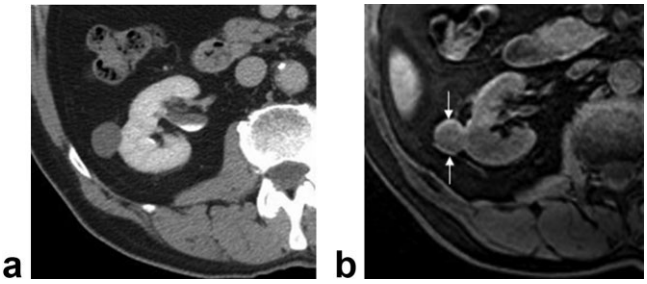

Figure 1. **a:** A right renal cyst shows water attenuation and a thin imperceptible wall by CT (cropped from an enhanced, nephrographic phase CT image, helical acquisition = 512 × 512, slice thickness = 5 mm, FOV = 50 cm) showing apparent wall thickening on (**b**) an axially-reconstructed T1-weighted 3D FS SPGR image (FOV = 36 × 36 cm, 320 × 160 × 40, effective "slice" thickness = 3 mm, TR/TE = 3.3/1.6 msec, flip angle [FA] = 12°).

We have observed that renal lesions that meet criteria for a simple cyst on other modalities, such as ultrasound and CT, sometimes demonstrate increased wall thickness on MRI. This raises the suspicion for a complicated cyst. The problem is illustrated in Figs. 1 and 2, where cysts that are simple by CT (Fig. 1a) or ultrasound (Fig. 2a) criteria appear thick-walled on MR images (Figs. 1b and 2b). This observation is confirmed by a recent study of cystic renal masses, in which increased observed wall thickness on MRI was often a reason for "upgrading" cystic renal lesions (7).

We propose that the apparent wall thickening seen in clinical images can sometimes be produced due to the low resolution employed in standard clinical imaging, resulting in the characteristic Gibbs ringing, most intense at the borders of the object, i.e., the cyst wall. Low signal-to-noise ratio (SNR) along with standard data filtration techniques employed can further mask the internal ringing in the cyst, leaving only a prominent cyst wall. This point is illustrated in this study with a simple simulation, and on cysts imaged at varying resolutions to demonstrate that the apparent wall thickening often is, in fact, artifactual.

MATERIALS AND METHODS

Simulated k-space data for a 4-cm cyst were created in a 40 cm field of view (FOV) image (512 × 512 native resolution) in MATLAB (The Mathworks, Natick, MA, USA). Additional k-space data sets were created using the central 256 × 256 and 256 × 128 points. A noise-free profile across the low-resolution axis of the 256 × 128 image was obtained. The effect of data truncation and concomitant Gibbs ringing was observed on a noise-free projection across the low-resolution axis of the 256 × 128 image. The effect of superimposed noise (simulated such that SNR was approximately 20) on the appearance of the wall was also observed.

Next, the effect of filtration on cyst wall appearance was studied. Noise was simulated in the three aforementioned images, such that "cyst" SNR was approximately 7, 14, and 20 for the three images, respectively. Noise-free images and a 256 × 128 image with SNR = 10 were also created for comparison purposes. Actual cyst wall thickness was set at 0.25 mm, and the ratio of cyst water to cyst wall signal was set at 1:4, based on crude empirical observation. An inverse 2D fast Fourier transform (FFT) yielded simulated images. A Fermi filter (radius = one-half of the matrix size, transition width = 10 pixels) was applied to reduce ringing, to simulate the norm on GE (General Electric Medical Systems, Milwaukee, WI, USA) scanners, which were used to acquire a majority of our clinical images. Images/profiles were examined for wall thickening. The effect of Gibbs ringing combined with data filtration (i.e., the Fermi filter) designed to suppress small undulations in the data was illustrated on noise-free 256 × 256 matrix images and profiles across them, with and without application of a Fermi filter. The effect of noise when combined with filtration on low-resolution images was illustrated on a 256 × 128 filtered image with SNR = 20, as compared to a identical image but with an SNR = 10. Finally, the effect of increasing resolution on such images was studied by comparing the images and profiles from the 512 × 512, 256 × 256, and 256 × 128 data sets.

The clinical portion of this study was approved by the institutional review board (IRB) at the institution where this study was conducted. Based on theoretical analysis, a protocol was implemented in which patients who show cyst wall thickness on the preliminary standard MRI imaging sequences are scanned at progressively higher resolutions through the kidneys. This allows separation of artifactual from true wall thickening. The cystic lesions studied here were identified prospectively prior to contrast on a routine MRI liver or renal mass

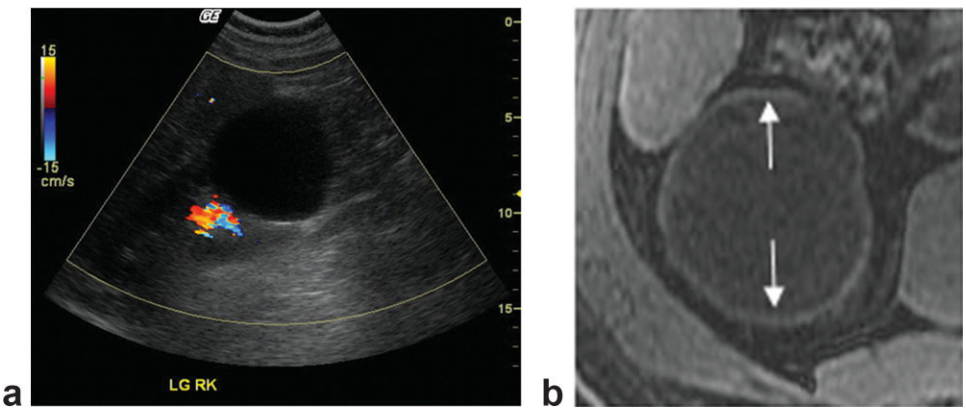

Figure 2. **a:** A right renal cyst, anechoic, with no internal flow and a thin, imperceptible wall by ultrasound, showing apparent wall thickening on (**b**) an axial T1-weighted 2D SPGR image (FOV = 40 × 30 cm, 512 × 160, slice thickness = 6 mm, TR/TE = 190/1.7 msec, flip angle [FA] = 70°).

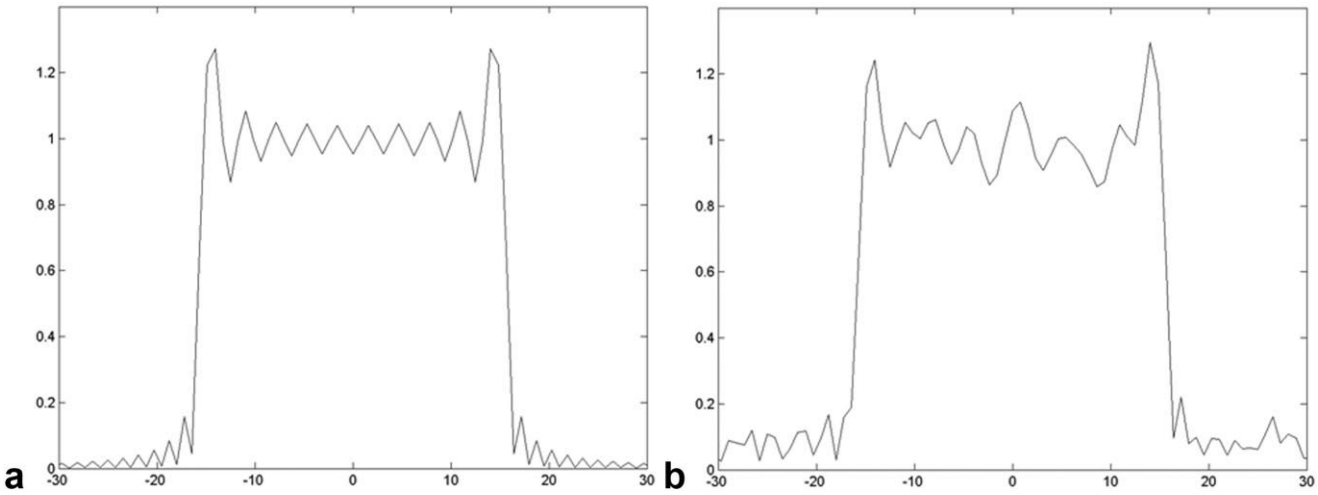

Figure 3. Profile across an ideal circular object with (**a**) data truncated at 256 × 256, but with no noise effects and (**b**) same matrix but with noise in the data. The edges are accentuated but the characteristic signal fluctuations of the Gibbs artifact are more difficult to spot in (b). Horizontal axes are marked as millimeter (mm) distance from the center of the images. Vertical axes represent signal intensity in arbitrary units.

examination, acquired with an 8-channel phased-array coil, and sequences consisting minimally of coronal single-shot T2-weighted fast spin-echo (FSE), axial fat-saturated (FS) T2-weighted FSE, axial FS two-dimensional (2D) spoiled gradient-echo (SPGR), and axial or coronal FS 3D SPGR precontrast and postcontrast. Seven patients were identified on the scanner as having thick walls (>3 mm) on one or more of the precontrast scans, but with no focal nodularity or other characteristics to suggest malignancy. In each case, this wall thickening was seen on FS SPGR sequences. Six of the patients had been scanned on a GE 1.5T Signa scanner, and one patient had been scanned on a Philips 3.0T Intera scanner (Philips Medical Systems North America, Bothell, WA, USA). The images depicted in this study were acquired with: a 2D FS SPGR sequence, TR/TE = 135 msec/1.3 msec, NEX = 1, slice thickness = 6 mm, and data matrices = 256 × 128 and 256 × 256. FOV varied from 38 to 40 cm^2, depending on the patient. Four patients were able to provide breath-holds long enough (30–32 seconds, depending on the patient) for an additional 512 × 512 acquisition. Cyst wall thickness was measured at each of the three resolutions, and the means were compared to each other via a two-tailed Student's *t*-test. A *P* value of less than 0.01 was considered statistically significant.

RESULTS

Simulation Study

Figure 3 depicts profiles across the simulated idealized circular object, without (Fig. 3a) and with (Fig. 3b) the effects of noise, across a 256 × 256 simulated image. Please note that for all examples shown here, the images have been cropped to highlight the cyst, and the entire image is not shown. Figure 4 depicts the effect of filtration. Simulated 256 × 256 images without (Fig. 4a) and with Fermi filtration (Fig. 4b) are shown, along with corresponding profiles across these images (Fig. 4c and d, respectively). The effect of noise on filtered images is depicted in Fig. 5, which shows 256 × 128 matrix simulated cyst images with an SNR = 20 (Fig. 5a) and 10 (Fig. 5b). The corresponding profiles across the low-resolution direction are shown in Fig. 5c and d, respectively. Finally, the effect of increasing resolution on the apparent wall thickness can be seen in Fig. 6, which shows 256 × 256 (Fig. 6a) and 512 × 512 (Fig. 6b) images across the simulated cyst. The profiles across these images are shown in Fig. 6c and d, respectively. These images and profiles can be compared to their counterparts in Fig. 5a and c, which are the corresponding 256 × 128 low-resolution image and profiles.

Clinical Study

Figures 7 and 8 depict exophytic renal cysts from patients, acquired at 256 × 128 (Figs. 7a and 8a), 256 × 256 (Figs. 7a and 8b), and 512 × 512 matrices (Figs. 7c and 8c), and show the effect of resolution and Gibbs artifact on apparent wall thickness on two patients with exophytic renal cysts. The FOV is identical for all three images in each figure. The average wall thicknesses in the phase-encoding direction for the 256 × 128 (group 1), 256 × 256 (group 2), and 512 × 512 (group 3) images, were 4.0 ± 0.9 mm ($N = 7$), 2.3 ± 0.6 mm ($N = 7$), and 1.2 ± 0.5 mm ($N = 4$), respectively. The difference in wall thickness was statistically significant ($P < 0.01$) for all cases ($P = 0.003$ for group 1 compared to group 2; $P = 0.007$ for group 1 compared to group 3; and $P = 0.001$ for group 2 compared to group 3).

DISCUSSION

The effects of data truncation on MR images are a well known and long understood phenomena (16–19). In standard Fourier imaging, it is assumed that the acquired MR data are in good approximation, the inverse Fourier transform of the spin density, or desired image.

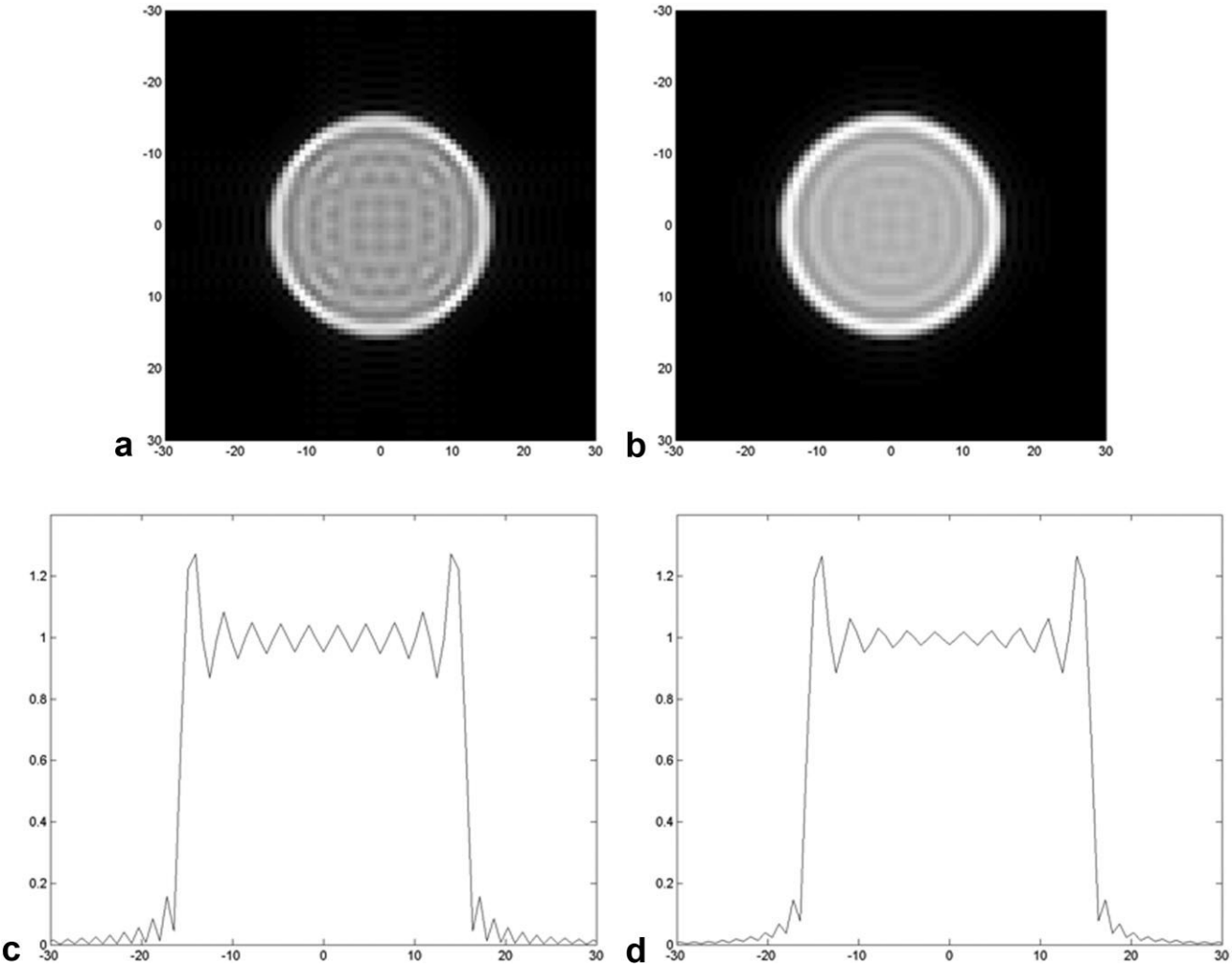

Figure 4. Effect of filtration on cyst wall characteristics. Simulated 4-cm cyst in a 40-cm FOV, (**a**) 256 × 256 image without filtration, and (**b**) 256 × 256 image with application of a Fermi filter. No noise has been added to these images. Axes are marked as millimeter (mm) distance from the center of the image. Profiles across the (**c**) unfiltered and (**d**) filtered images show the accentuation of the wall and the dampening of the intensity of the rings relative to each other, due to filtering. Horizontal axes are marked as mm distance from the center of the images. Vertical axes represent signal intensity in arbitrary units.

This would be true if k-space is perfectly and infinitely sampled. However, in practice, not all of k-space is sampled. Typically, for example, a central portion of k-space (which contains most of the signal energy) is sampled with a desired density, while the periphery is assumed to be filled with zeros. The collected data are thus truncated, representing the complete Fourier data windowed by a rect function. This has consequences for the appearance of the image. When there is an abrupt change in spin density between two adjacent structures, the result is an oscillating overshoot and undershoot in the signal intensity, termed truncation artifact, and the ringing pattern that is seen in the image is often called Gibbs ringing. Increasing the number of points N used to sample a given direction (while keeping the step size in k-space constant) increases the number of oscillations while decreasing their width. For a large enough N, the oscillations become so close together that they are essentially not detectable. The value of the overshoot and undershoot is approximately 9% of the step-size between the two spin densities. Importantly, the maximal overshoot and undershoot remain the same regardless of N, even while the width of the interface between two entities with different signal characteristics decreases with N (16,17).

As expected, apparent thickening of the border of the simulated phantom cysts is seen in the lower resolution data sets (Fig. 3a), accentuated in the direction(s) reconstructed with a smaller number of data points. However, in the absence of noise, the characteristic undulations due to the Gibbs ringing (16,17) are easy to spot without the effects of noise, making it clear that this wall thickening is indeed due to data truncation. The addition of noise leaves a thick edge due to the large side lobes of the object, but the undulations are harder to discern (Fig. 3b). This translates to an apparently thick wall in the low-resolution direction.

The filtration commonly applied in MRI by most, if not all vendors, can also confound interpretation. Typically, a filter such as the Fermi filter demonstrated here (Fig.

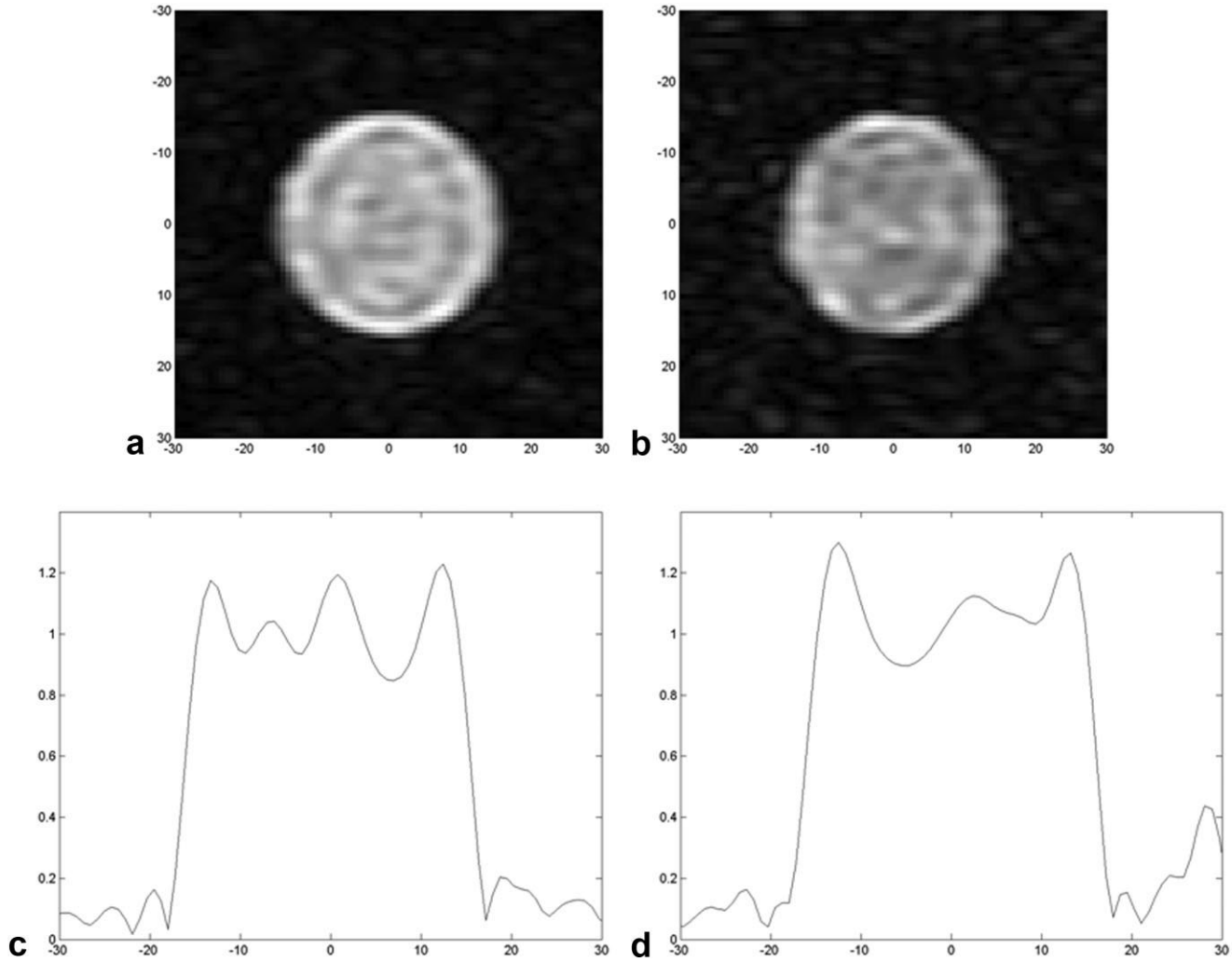

Figure 5. The combined effect of filtering and noise on cyst wall characteristics. Simulated 4-cm cyst in a 40-cm FOV, with a Fermi filter. (**a**) 256 × 128 image with SNR simulated as approximately 20, and (**b**) 256 × 128 image with SNR simulated as approximately 10. Axes are marked as millimeter (mm) distance from the center of the image. Profiles across the (**c**) high SNR and (**d**) low SNR images show the accentuation of the wall due to filtering and noise. Horizontal axes are marked as mm distance from the center of the images. Vertical axes represent signal intensity in arbitrary units.

4), is employed to reduce the effect of ringing in MR images, serving to dampen the rings in the images. However, in noisy images, this dampening of the ringing is made more difficult to discern, further accentuating the apparently thickened wall (Fig. 5). Thus the combination of truncation, filtration, and noise can create the situation in which a simple cyst can have an apparently thick wall on MR images.

Figures 7 and 8 show the effect of resolution, truncation artifact, and noise on apparent wall thickness in two patients with exophytic renal cysts. At lower resolutions, walls of the depicted renal cysts show marked thickness, particularly in the phase-encode direction at the lowest resolution. As in-plane resolution increases, the wall becomes markedly less thickened in appearance, nearly disappearing at the highest resolutions acquired. This effectively proves that the wall thickness seen on the typical clinically-acquired, relatively low-resolution images (Figs. 5a and 6a) is in fact artifactual, and, as shown by the simulations and experiments, that this is likely due to a combination of data truncation, filtration, and SNR considerations. This observation is quantitatively confirmed, as the observed wall thickness is significantly decreased as resolution increases. The decrease in apparent thickness is slightly less than the proportional increase in resolution in each case. This is probably due to two factors. First, as resolution improves, the wall thickness becomes so small that the measurement is progressively more difficult to make. This is reflected in the progressively larger error bar in the measurements (as a percentage of the measured thickness) in the higher-resolution data sets. Second, the measured wall thickness approaches the true wall thickness due to improved resolution, leading to a less than proportional decrease in the measured wall thickness.

One weakness in this study is the small number of patients with renal cysts ($N = 4$) that were scanned at the highest resolution (512 × 512 matrix). This is because long breathhold times are required to obtain

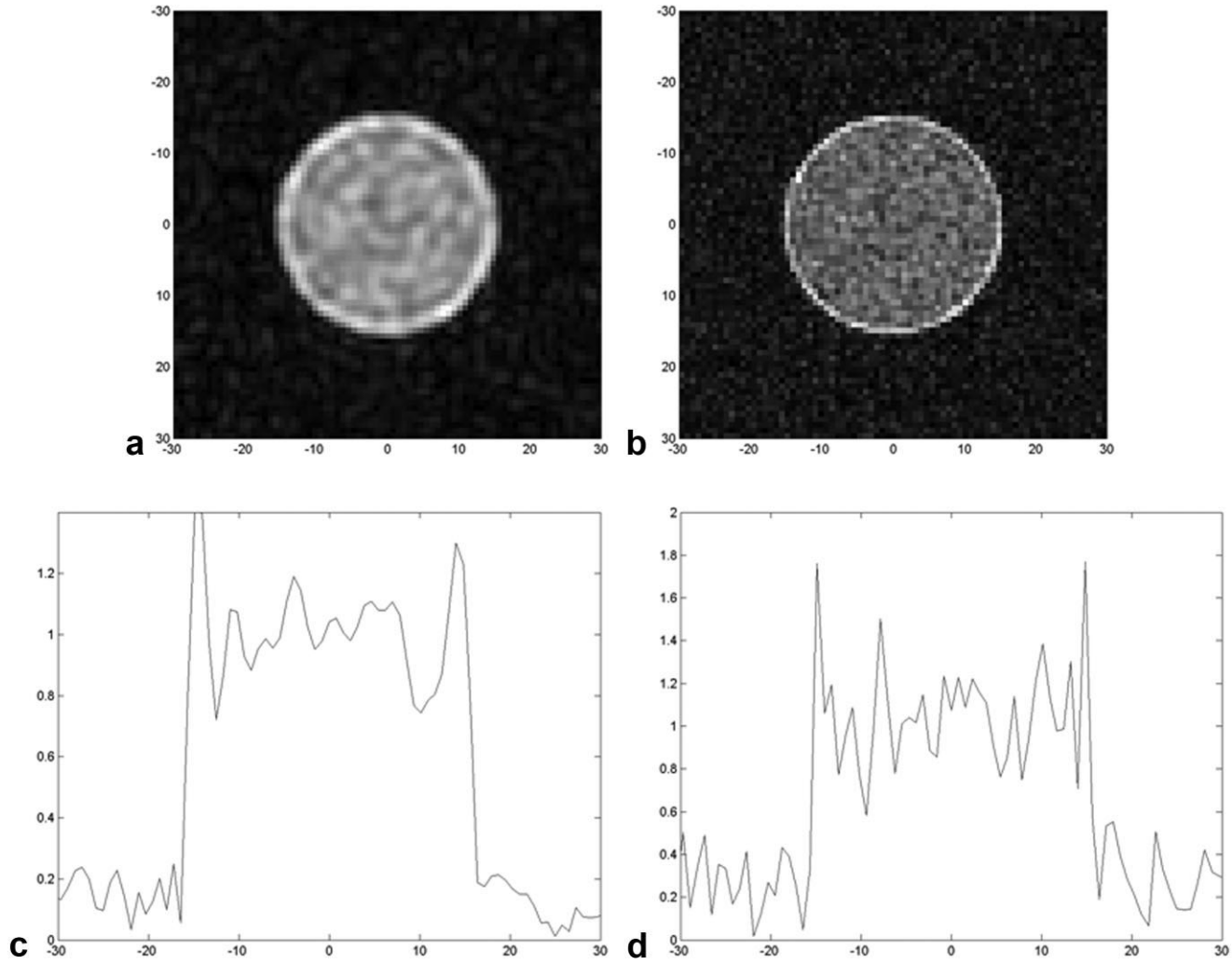

Figure 6. The effect of resolution on apparent cyst wall thickness with filtering and noisy data. Simulated images of a 4-cm cyst in a 40-cm FOV, with a Fermi filter applied. Noise levels were kept constant, and are the same as in the image in Fig. 5a. The decrease in SNR is due to increasing resolution. (**a**) 256 × 256 image with SNR simulated as approximately 14, and (**b**) 512 × 512 image with SNR simulated as approximately 7. Axes are marked as millimeter (mm) distance from the center of the image. Profiles across the (**c**) intermediate-resolution and (**d**) high-resolution images show the decreasing apparent wall thickness with improved resolution. Horizontal axes are marked as mm distance from the center of the images. Vertical axes represent signal intensity in arbitrary units.

these images, and not all patients were able to comply with this request. However, even the comparison between the 256 × 256 and 256 × 128 data sets is sufficient to illustrate the point of this study, as the difference between these two groups is statistically significant. Second, the signal assigned to the wall and cyst contents in the simulations was based on empirical observations from clinical images, rather than quanti-

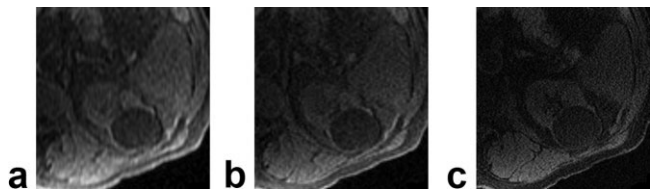

Figure 7. Patient with a renal cyst showing artifactual wall thickening that resolves upon high-resolution imaging. The above are cropped from 2D FS SPGR data sets, FOV = 38 cm, flip angle (FA) = 70°, TR/TE = 135 msec/1.3 msec, number of excitations (NEX) = 1, slice thickness = 6 mm, and matrices of (**a**) 256 × 128, (**b**) 256 × 256, and (**c**) 512 × 512.

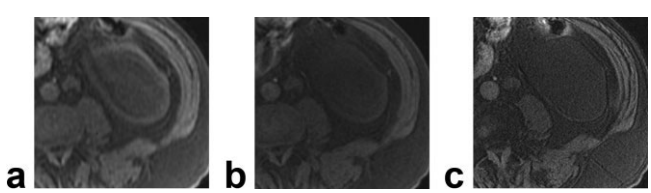

Figure 8. Another patient with a renal cyst showing artifactual wall thickening that resolves upon high-resolution imaging. The above are cropped from 2D FS SPGR data sets, FOV = 38 cm, flip angle (FA) = 70°, TR/TE = 135 msec/1.3 msec, number of excitations (NEX) = 1, slice thickness = 6 mm, and matrices of (**a**) 256 × 128, (**b**) 256 × 256, and (**c**) 512 × 512.

tative relaxation parameter measurements. However, the purpose of the simulations is to simplify and understand the various facets of the problem, for which these simple simulations are more than sufficient.

In the evaluation of renal cystic lesions, our clinical experience and these results show that Gibbs artifacts lead to an apparent increase in the lesion wall thickness in the phase-encoding direction (because it is usually the lower-resolution direction) of an otherwise simple cyst. This finding has important clinical implications in the management of cystic renal masses as unnecessary imaging follow-up may be performed on simple renal cysts. If a lesion depicting wall thickness on MR images is encountered, image interpretation should take into account the direction of wall thickening. Ideally images at higher resolution should be obtained as this will lead to narrowing of the Gibbs bands and thus allow differentiation of truly thick walls from artifactual complexity (as illustrated in Figs. 7 and 8). Gibbs ringing can be reduced by using a variety of techniques in addition to filtration, including prior information-based methods, and data extrapolation methods (20–24). However, these methods require offline signal processing, which is not practical for day-to-day clinical imaging. Thus the simplest method, i.e., obtaining high-resolution images to prove that wall thickening is artifactual, is also the most preferable. This method does have a downside in that the potentially confounding lesion must be identified while the patient is on the scanner, which can be difficult in many clinical situations.

An argument could be made that an experienced MR reader will ignore this artifactual wall thickness because he/she instinctively realizes that the appearance encountered is not "real," either due to force of experience or due to correlation with the numerous other sequences in the examination, particularly the T2-weighted imaging. While this argument carries an element of truth, it is worth keeping the factors illustrated in this study in mind while ignoring probable apparent wall thickness, so that one understands what is being ignored and why. Moreover, in our experience not all MR readers (even body/MRI experts) are necessarily experienced or confident enough that such a conclusion is automatic, and it is hoped that the present study can help them as well.

The issue of whether or how to adopt the Bosniak CT criteria for MR is one that has important implications in the day-to-day management of cystic renal masses. The Bosniak system has been discussed extensively in the literature, and will not be reviewed here. However, the application of this classification system to MRI may pose limitations that are MRI specific. As this study has shown, wall thickness, for example, as a criterion for determining the complexity of a cystic lesion on MR must be interpreted with caution in the context of the number of phase-encoding steps of the scan, to avoid upgrading a simple renal cyst with an imperceptible or hairline thin wall on ultrasound and CT (Bosniak I or II) to a complicated cyst (Bosniak IIF, likely benign, but in need of follow-up imaging). The calcifications in the cyst wall or septation are easily seen on CT, as opposed to MRI, though this finding is less important compared to enhancement (6,7,25). There is one study in the literature in which an attempt was made to correlate each individual Bosniak criterion on MRI with malignancy (9). While the number of subjects and complex cystic lesions (37 and 55, respectively) included in the study were relatively small, the researchers found that mural thickness, nodularity, and enhancement were all correlated with malignancy, providing preliminary results that confirm some of the Bosniak criteria. On the other hand, in this study, all Category II and III lesions were benign, and 14 of 32 Category IV lesions were malignant. This differs from the predicted results from the Bosniak system, which suggest that half (or at least some) Category III lesions should be malignant, and almost all Category IV lesions should be cancerous. However, the small number of cases, along with lack of separation into Category IIF may serve as limitations of the study. A future multicenter study with a large number of patients, in which each individual Bosniak criterion (for MRI) is evaluated against malignancy, along with the evaluation of the various Bosniak categories as predictors of malignancy, would be quite useful in both application of the system and identification of caveats to MRI.

In conclusion, this work shows that the thickness of renal cystic lesions can show apparent thickening on MRI due to a combination of data truncation, filtration, and SNR effects. The Bosniak criterion of a "thin, imperceptible wall" of a simple cyst should therefore be applied carefully in MRI of renal cystic lesions. Artifactual wall thickening can be easily confirmed on individual patients by adding sequences to the examination that include higher-resolution imaging, and this step can save the patient unnecessary imaging follow-up.

ACKNOWLEDGMENTS

This work is dedicated to the memory of Dr. Saroja Adusumilli. We thank Drs. Mark Griswold and Sherif Nour of Case Western Reserve University for helpful discussions and comments on the manuscript. V. Gulani was supported in part by CTSA, grant number 1KL2RR024990.

REFERENCES

1. Levy P, Helenon O, Merran S, et al. [Cystic tumors of the kidney in adults: radio-histopathologic correlations]. J Radiol 1999;80:121–133.
2. Kim JC, Kim KH, Lee JW. CT and US findings of multilocular cystic renal cell carcinoma. Korean J Radiol 2000;1:104–109.
3. Hartman DS, Davis CJ Jr, Johns T, Goldman SM. Cystic renal cell carcinoma. Urology 1986;28:145–153.
4. Bosniak MA. The current radiological approach to renal cysts. Radiology 1986;158:1–10.
5. Israel GM, Bosniak MA. Renal imaging for diagnosis and staging of renal cell carcinoma. Urol Clin North Am 2003;30:499–514.
6. Israel GM, Bosniak MA. MR imaging of cystic renal masses. Magn Reson Imaging Clin N Am 2004;12:403–412.
7. Israel GM, Hindman N, Bosniak MA. Evaluation of cystic renal masses: comparison of CT and MR imaging by using the Bosniak classification system. Radiology 2004;231:365–371.
8. Israel GM, Bosniak MA. How I do it: evaluating renal masses. Radiology 2005;236:441–450.
9. Balci NC, Semelka RC, Patt RH, et al. Complex renal cysts: findings on MR imaging. AJR Am J Roentgenol 1999;172:1495–1500.

10. Bosniak MA. Difficulties in classifying cystic lesions of the kidney. Urol Radiol 1991;13:91–93.
11. Bosniak MA. Diagnosis and management of patients with complicated cystic lesions of the kidney. AJR Am J Roentgenol 1997;169: 819–821.
12. Bosniak MA. The use of the Bosniak classification system for renal cysts and cystic tumors. J Urol 1997;157:1852–1853.
13. Bosniak MA. Problems in the radiologic diagnosis of renal parenchymal tumors. Urol Clin North Am 1993;20:217–230.
14. Israel GM, Bosniak MA. Follow-up CT of moderately complex cystic lesions of the kidney (Bosniak category IIF). AJR Am J Roentgenol 2003;181:627–633.
15. Hartman DS, Choyke PL, Hartman MS. A practical approach to the cystic renal mass. Radiographics 2004;24:S101–S115.
16. Haacke EM, Brown RW, Thompson MR, Venkatesan R. Magnetic resonance imaging: physical principles and sequence design. New York: John Wiley & Sons, 1999. 914 pp.
17. Liang Z-P, Lauterbur PC. Principles of magnetic resonance imaging: a signal processing perspective. New York: IEEE Press, 2000. 416 pp.
18. Lufkin RB, Pusey E, Stark DD, et al. Boundary artifact due to truncation errors in MR imaging. AJR Am J Roentgenol 1986;147: 1283–1287.
19. Wood ML, Henkelman RM. Truncation artifacts in magnetic resonance imaging. Magn Reson Med 1985;2:517–526.
20. Martin JF, Tirendi CF. Modified linear prediction modeling in magnetic resonance imaging. J Magn Reson 1989;82:392–399.
21. Amartur S, Liang ZP, Boada F, Haacke EM. Phase-constrained data extrapolation method for reduction of truncation artifacts. J Magn Reson Imaging 1991;1:721–724.
22. Barone P, Sebastiani G. A new method of magnetic resonance image reconstruction with short acquisition time and truncation artifact reduction. IEEE Trans Med Imaging 1992;11:250–259.
23. Liang Z-P, Boada FE, Constable RT, et al. Constrained reconstruction methods in MR imaging. Rev Magn Reson Med 1992;4:67–185.
24. Placidi G, Sotgiu A. A novel algorithm for the reduction of undersampling artifacts in magnetic resonance images. Magn Reson Imaging 2004;22:1279–1287.
25. Israel GM, Bosniak MA. Calcification in cystic renal masses: is it important in diagnosis? Radiology 2003;226:47–52.